Eur. Phys. J. D **32**, 9–17 (2005)
DOI: 10.1140/epjd/e2004-00143-x

THE EUROPEAN PHYSICAL JOURNAL D

On the low-velocity limit of the Bohr stopping formula

M.M. Basko[1,2,a]

[1] Institute for Theoretical and Experimental Physics, B. Cheremushkinskaya 25, 117218 Moscow, Russian Federation
[2] Max-Planck-Institut für Quantenoptik, Hans-Kopfermann-Str. 1, 85748 Garching, Germany

Received 2nd July 2004
Published online 26 October 2004

Abstract. The low-velocity limit of the classical Bohr stopping model is investigated by applying non-perturbative methods. For the repulsive Coulomb interaction between a heavy projectile and a harmonically bound electron, the stopping cross-section $S_+(v)$ is found to scale as $v^{5/3}$ in the limit of $v \to 0$, where v is the projectile velocity. This scaling is obtained by establishing a corresponding scaling law for the energy transfer $T_+(v,b)$ in a single collision with an impact parameter b, namely, that $T_+/v^{1/3}$ is a function of a scaled variable $b/v^{2/3}$. For the opposite case of the Coulomb attraction, direct numerical calculations reveal that the energy transfer $T_-(v,b)$ exhibits sharp resonances along the b axes when v becomes sufficiently small. The latter results in a characteristic non-regular behaviour of $S_-(v)$ near maximum. Suitable fitting formulae are proposed for the corresponding stopping numbers $L_\pm(v)$.

PACS. 34.50.Bw Energy loss and stopping power – 52.40.Mj Particle beam interactions in plasmas

1 Introduction

The famous Bohr formula [1],

$$\frac{dE}{dx} = -\frac{4\pi Z_1^2 e^4}{mv^2}\, n_e \ln\frac{C_B\, mv^3}{|e^2 Z_1|\omega}, \qquad (1)$$
$$C_B = \frac{2}{\exp(\gamma)} = 1.1229,$$

($\gamma = 0.577\ldots$ is the Euler's constant) for the energy loss by a fast point-like charge $Z_1 e$ moving with a non-relativistic velocity v through neutral matter was derived on the basis of a simple (but very fruitful) classical model: the projectile $Z_1 e$ looses its energy in random collisions with electrons (charge $-e$, mass m) bound harmonically in classical oscillators with an eigenfrequency ω. In the simplest case, a heavy projectile is considered, whose mass $M_1 \gg m$ does not enter the expression for the stopping force. Evidently, the Bohr formula (1) can only be used for

$$v > v_s = \left(\frac{|Z_1 e^2|\,\omega}{m}\right)^{1/3}, \qquad (2)$$

where it represents the first term in the asymptotic expansion with respect to a large parameter v/v_s.

With the advent of quantum mechanics, the applicability of the Bohr formula was restricted by the condition

$$\alpha_v = \frac{|e^2 Z_1|}{\hbar v} \gg 1 \qquad (3)$$

of not too high projectile velocities. In addition, the oscillator frequency ω was replaced by the mean atomic frequency $\langle\omega\rangle$ defined as

$$Z_2 \ln\langle\omega\rangle = \sum_n f_n \ln\omega_n, \qquad (4)$$

where Z_2 is the atomic number of the target atom, ω_n and f_n are the frequencies and oscillator strengths of the dipole transitions from the ground state [2,3]. Ironically, the behaviour of the Bohr stopping force in the limit of low velocities, $v \ll v_s$, appears to have remained unknown until now.

In his original work [1] Bohr derived equation (1) for $v \gg v_s$ by combining two asymptotic expressions for the energy transfer $T(b)$ at a given impact parameter b, namely, $T_d(b)$ for distant collisions obtained in the dipole approximation for a perturbed oscillator, and the Rutherford value $T_R(b)$ for close collisions, where the oscillator binding can be ignored. Recently Sigmund [4] proposed to extend Bohr's calculation to $v < v_s$ in a straightforward manner, by calculating the crossover point $b = b_\times$ between $T_d(b)$ and $T_R(b)$ and applying either of them in the corresponding region. One can hardly expect that such a procedure would lead to a correct answer because both expressions for $T(b)$, calculated by Bohr within a perturbative approach for $v \gg v_s$, become inapplicable at $v < v_s$.

Here, in contrast to reference [4], a non-perturbative analysis is applied. It is found that the two cases of the repulsive and attractive interaction between the projectile and the target electron are qualitatively and quantitatively quite different (the Barkas effect). For the repulsion

[a] e-mail: basko@itep.ru

case, it is shown that the stopping cross-section S_+ becomes asymptotically proportional to $v^{5/3}$ as $v \to 0$ (cf. $S_\pm \propto v^{3.3}$ in Ref. [4]). The numerically calculated values of the stopping number $L_\pm(v)$ are approximated by suitable analytical formulae.

The present results for the low-velocity Bohr stopping power of charged particles may be of particular interest for antiprotons and other antinuclei decelerated in ordinary matter because no recombination occurs onto antinuclei at low velocities.

2 Parametrization of the problem

In the binary collision approach, the stopping force $-dE/dx$ is often expressed in terms of the stopping cross-section

$$S = -\frac{1}{n_e}\frac{dE}{dx} \tag{5}$$

(per one electron in our case), which can be calculated as an integral

$$S = 2\pi \int_0^\infty T(b)\, b\, db \tag{6}$$

of the energy transfer $T(b)$ in a single collision with an impact parameter b.

In the Bohr model, the stopping cross-section S for a heavy projectile ($M_1 \gg m$) can only be a function of the following four dimensional parameters,

$$Z_1 e^2, \quad m, \quad \omega, \quad v. \tag{7}$$

The product $Z_1 e^2$ of the projectile and electron charges can be either positive (Coulomb repulsion) or negative (Coulomb attraction). One can choose the first three of these parameters — all having independent dimensions — as a basis for a new system of units, which is particularly suitable for the problem considered here. Then, the units of length, time and mass become

$$[l] = b_s = \left(\frac{\left|Z_1 e^2\right|}{m\omega^2}\right)^{1/3}, \quad [t] = \omega^{-1}, \quad [m] = m; \tag{8}$$

the unit of velocity, $v_s = b_s\omega$, is given by equation (2); the unit of the stopping cross-section is given by

$$[S] = m v_s^2\, b_s^2 = \frac{Z_1^2 e^4}{m v_s^2}. \tag{9}$$

For $Z_1 = 1$ and $\hbar\omega = 2$ Ry our units coincide with the atomic units. Below, when given in units (8), the physical quantities are marked with a bar.

Clearly, the dimensionless stopping cross-section $\bar{S} = S/[S]$ is a universal function of only one variable — the dimensionless velocity $\bar{v} = v/v_s$. More precisely, there are two functions, $\bar{S}_+(\bar{v})$ and $\bar{S}_-(\bar{v})$, corresponding to the two possible signs of the product $Z_1 e^2$. Based on the high-velocity limit, the functions $\bar{S}_\pm(\bar{v})$ are usually cast in the form

$$\bar{S}_\pm(\bar{v}) = 4\pi\, \bar{v}^{-2}\, L_\pm(\bar{v}), \tag{10}$$

where $L_\pm$ becomes the Coulomb logarithm at $\bar{v} \gg 1$. Earlier, such dimensional considerations have been formulated in a somewhat different form by Lindhard [5]. Often (as, for example, in Ref. [4]) the parameter $\xi = \bar{v}^3$ is used instead of $\bar{v}$.

3 Bohr's solution for $v \gg v_s$

Bohr [1] calculated the leading term in the asymptotic expansion of $\bar{S}_\pm(\bar{v})$ for $\bar{v} \gg 1$, namely

$$L_+(\bar{v}) = L_-(\bar{v}) = \ln\left(C_B\, \bar{v}^3\right). \tag{11}$$

More specifically, he observed that for collisions with impact parameters $\bar{b} \gg \bar{b}_0 = \bar{v}^{-2}$ one can apply a dipole approximation and calculate

$$\bar{T}(\bar{b}, \bar{v}) = \bar{T}_d(\bar{b}, \bar{v}) = \frac{2}{\bar{v}^4}\left[K_0^2\left(\frac{\bar{b}}{\bar{v}}\right) + K_1^2\left(\frac{\bar{b}}{\bar{v}}\right)\right], \tag{12}$$

whereas for $\bar{b} \ll \bar{b}_{ad} = \bar{v}$ one can ignore the oscillator binding and use the Rutherford scattering result

$$\bar{T}(\bar{b}, \bar{v}) = \bar{T}_R(\bar{b}, \bar{v}) = \frac{2\bar{v}^2}{1 + (\bar{b}\bar{v}^2)^2}; \tag{13}$$

here $K_0(x)$ and $K_1(x)$ are the modified Bessel functions in the usual notation [6]. In conventional units, the impact parameter b_0 of scattering by 90°, and the adiabatic (dynamic screening) radius b_{ad} are given by

$$b_0 = \frac{\left|Z_1 e^2\right|}{m v^2}, \quad b_{ad} = \frac{v}{\omega}. \tag{14}$$

Bohr's calculation has revealed that for $\bar{v} \gg 1$ the main contribution to the stopping cross-section S comes from the impact parameter range $b_0 \lesssim b \lesssim b_{ad}$, where both the dipole approximation and that of the free Rutherford scattering are valid. We will see that in the opposite limit of $\bar{v} \ll 1$ the dominant contribution to S comes from the range of b values, where none of these approximations is applicable.

Much of the subsequent analysis will be based on a distinction between the adiabatic and non-adiabatic collisions. In adiabatic collisions, occurring at $b > b_{ad}$, the characteristic timescale Δt_c of variation of the external force acting on the harmonically bound electron is larger than ω^{-1}. Expression (12) tells us that the energy transfer in the adiabatic collisions is exponentially small, i.e.

$$\bar{T}(\bar{b}, \bar{v}) \approx \frac{2\pi}{\bar{v}^3 \bar{b}} \exp\left(-2\bar{b}/\bar{b}_{ad}\right). \tag{15}$$

4 Non-perturbative approach

In classical mechanics, the collision of a heavy point charge with a harmonically bound electron is described by two

relatively simple equations of motion

$$\ddot{\bar{x}} = -\bar{x} + \delta_1 \frac{\bar{x} - \bar{v}\bar{t}}{\bar{R}^3}$$

$$\ddot{\bar{y}} = -\bar{y} + \delta_1 \frac{\bar{y} + \bar{b}}{\bar{R}^3}, \tag{16}$$

where the double dot denotes the second derivative with respect to $\bar{t}$,

$$\delta_1 = \begin{cases} +1, \, Z_1 e^2 > 0, \\ -1, \, Z_1 e^2 < 0, \end{cases} \tag{17}$$

and

$$\bar{R} = \left[(\bar{x} - \bar{v}\bar{t})^2 + (\bar{y} + \bar{b})^2 \right]^{1/2} \tag{18}$$

is the distance between the electron and the projectile. It is assumed that the collision occurs in the (x, y)-plane, with $x(t)$, $y(t)$ being the coordinates of the electron as measured with respect to the motionless oscillator center. The projectile moves along the x-axis and has the coordinates $\{x_p, y_p\} = \{vt, -b\}$, where b is the impact parameter with respect to the oscillator center.

Here an idealized case is considered, where the binding force of the three-dimensional oscillator extends to infinity. Clearly, in such a case no charge transfer can occur. If the electron is at some time captured by the moving projectile, it will later be torn off by the infinitely growing oscillator force. Then, the energy transfer $\bar{T}$ in a single collision can be calculated by solving equations (16) with the initial conditions

$$\bar{x} = \dot{\bar{x}} = \bar{y} = \dot{\bar{y}} = 0 \tag{19}$$

at $\bar{t} = -\infty$, and evaluating

$$\bar{T}(\bar{v}, \bar{b}) = \frac{1}{2} \left(\bar{x}^2 + \dot{\bar{x}}^2 + \bar{y}^2 + \dot{\bar{y}}^2 \right) \tag{20}$$

at $\bar{t} = +\infty$. Despite certain technical difficulties, equations (16) can be solved numerically for most of the parameter range of practical interest, and the results of such calculations are presented below.

5 Adiabatic collisions

5.1 Equilibrium point

First of all consider collisions that occur in the adiabatic regime, i.e. at impact parameters $\bar{b} > \bar{b}_{ad}$. This will allow us to determine the value of $\bar{b}_{ad}$ for $\bar{v} \ll 1$.

In the course of a collision, the electron moves in a time-dependent potential

$$\bar{U}(\bar{t}, \bar{x}, \bar{y}) = \frac{1}{2}(\bar{x}^2 + \bar{y}^2) + \frac{\delta_1}{\bar{R}}, \tag{21}$$

where $\bar{R} = \bar{R}(\bar{t}, \bar{x}, \bar{y})$ is given by equation (18). If the collision is adiabatic, the electron stays in the immediate vicinity of the equilibrium point (e.p.), which corresponds to the local minimum of the potential (21) associated with

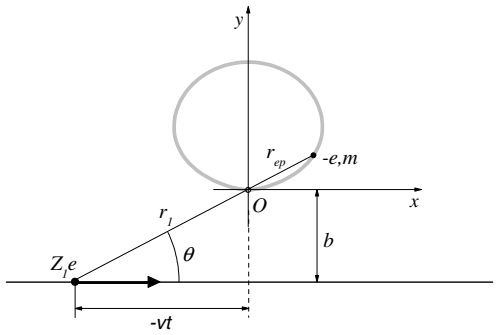

Fig. 1. Schematics of a collision between a projectile $Z_1 e$ and an electron $-e, m$ bound harmonically to the origin O of the coordinate system. Thick grey closed curve shows the trajectory of the equilibrium point for $\delta_1 = +1$, $\bar{b} = 0.5$.

$x = y = 0$ at $t = \pm\infty$. The trajectory of the e.p. is easily found to be given by

$$\bar{x}_{ep}(\bar{t}) = -\frac{\bar{v}\bar{t}}{\bar{r}_1} \varphi(\bar{r}_1),$$

$$\bar{y}_{ep}(\bar{t}) = \frac{\bar{b}}{\bar{r}_1} \varphi(\bar{r}_1), \tag{22}$$

where

$$\bar{r}_1 = \left(\bar{b}^2 + \bar{v}^2 \bar{t}^2 \right)^{1/2} \tag{23}$$

is the distance between the oscillator center and the projectile, and the dimensionless function $\varphi(\bar{r}_1)$ is defined by the equation

$$\varphi(\bar{r}_1 + \varphi)^2 = \delta_1. \tag{24}$$

Figure 1 shows an example of the e.p. trajectory for $\delta_1 = +1$; more details about the properties of function $\varphi(\bar{r}_1)$ are given in the Appendix.

For a fixed time $\bar{t}$, the potential (21) can be expanded in the vicinity of the e.p., which allows to calculate the two normal frequencies

$$\bar{\omega}_\parallel^2 = 1 + \frac{2\delta_1}{\left[\bar{r}_1 + \varphi(\bar{r}_1)\right]^3} = 1 + 2\delta_1 \left|\varphi(\bar{r}_1)\right|^{3/2}, \tag{25}$$

$$\bar{\omega}_\perp^2 = 1 - \frac{\delta_1}{\left[\bar{r}_1 + \varphi(\bar{r}_1)\right]^3} = 1 - \delta_1 \left|\varphi(\bar{r}_1)\right|^{3/2}, \tag{26}$$

of small oscillations around the e.p. The normal coordinates of these oscillations lie, respectively, along and perpendicular to the vector $\mathbf{r}_{ep} = \{x_{ep}, y_{ep}\}$.

Since in adiabatic collisions $|\varphi(\bar{r}_1)| = |\bar{\mathbf{r}}_{ep}| = \bar{r}_{ep}$ is essentially the displacement of the electron from its original position, and because the condition $|\varphi(\bar{r}_1)| \ll \bar{b}$ of applicability of the dipole approximation is equivalent to $\bar{b} \gg 1$, only adiabatic collisions with $\bar{b} \gg 1$ can be treated in the dipole approximation. For such collisions $\bar{\omega}_\parallel = \bar{\omega}_\perp = 1$, i.e. $\omega_\parallel = \omega_\perp = \omega$. For close adiabatic collisions with $\bar{b} \ll 1$ the dipole approximation is not applicable, and one has to take into account strong deviations of the eigenfrequencies (25), (26) from the unperturbed values $\bar{\omega}_\parallel = \bar{\omega}_\perp = 1$. This argument applies to adiabatic collisions at any collision velocity $0 < \bar{v} < \infty$.

Applicability of the dipole approximation to non-adiabatic collisions should, strictly speaking, be analyzed separately. For $\bar{v} \gg 1$ the answer is known: all collisions with $\bar{b} \gg \bar{v}^{-2}$ can be treated in the dipole approximation. As it will be clear from the subsequent analysis, the dipole approximation never applies to non-adiabatic collisions with $\bar{v} \lesssim 1$.

5.2 Criterion of adiabaticity

Now we want to determine the impact parameter b_{ad} separating adiabatic collisions from the non-adiabatic ones. For $\bar{v} \gg 1$ the answer is $\bar{b}_{ad} = \bar{v}$. To find b_{ad} for $\bar{v} \ll 1$, we need a general criterion for a collision to be adiabatic.

In the limit of an infinitely slow variation of the position $\mathbf{r}_{ep}(t)$ of the equilibrium point, the electron stays exactly at the local potential minimum $\mathbf{r} = \mathbf{r}_{ep}(t)$. A small acceleration $\ddot{\mathbf{r}}_{ep}$ of the equilibrium point causes a small deviation $|\mathbf{r} - \mathbf{r}_{ep}| \simeq \omega^{-2}|\ddot{\mathbf{r}}_{ep}|$ of the electron position from $\mathbf{r}_{ep}$; in adiabatic collisions this deviation should be small compared to r_{ep}. For anisotropic local oscillations around $\mathbf{r} = \mathbf{r}_{ep}$ with different normal frequencies $\omega_\parallel$ and $\omega_\perp$ this condition can be written as

$$\mu_\parallel = \frac{|\ddot{\bar{x}}_{ep}\,\cos\theta + \ddot{\bar{y}}_{ep}\,\sin\theta|}{\bar{\omega}_\parallel^2\,\bar{r}_{ep}} \ll 1, \tag{27}$$

$$\mu_\perp = \frac{|-\ddot{\bar{x}}_{ep}\,\sin\theta + \ddot{\bar{y}}_{ep}\,\cos\theta|}{\bar{\omega}_\perp^2\,\bar{r}_{ep}} \ll 1. \tag{28}$$

Here $0 < \theta < \pi$ is the angle between $\mathbf{r}_{ep}$ and x-axis (see Fig. 1), so that $\tan\theta = -b/vt$; the numerators in equations (27) and (28) contain the components of acceleration of the equilibrium point along the corresponding normal coordinates.

For any given $\bar{v}$, conditions (27) and (28) are always fulfilled at sufficiently large values of $\bar{b}$. The border value $\bar{b} = \bar{b}_{ad}$ between the adiabatic and non-adiabatic collisions corresponds to the case where either $\mu_\parallel$ or $\mu_\perp$ becomes comparable to 1. If we apply this criterion to the case of high velocities $\bar{v} \gg 1$, we find that $\mu_\parallel$, $\mu_\perp$ can be evaluated under the assumption that $\bar{r}_1 = \bar{b}/\sin\theta \gg 1$, when, according to equation (A.2), $\bar{r}_{ep} = |\varphi(\bar{r}_1)| = \sin^2\theta/\bar{b}^2$ and $\bar{\omega}_\parallel = \bar{\omega}_\perp = 1$. In this way we calculate

$$\mu_\parallel = \frac{\bar{v}^2}{\bar{b}^2}\,\sin^2\theta|6 - 9\sin^2\theta|, \quad \mu_\perp = \frac{\bar{v}^2}{\bar{b}^2}\,6\sin^3\theta|\cos\theta|, \tag{29}$$

and find that $\mu_\parallel$ is the first to reach the value of 1 at $\theta = \pi/2$ and $\bar{b} = \sqrt{3}\,\bar{v}$. Omitting the irrelevant factor of $\sqrt{3}$, we obtain the known result $\bar{b}_{ad} = \bar{v}$.

At low velocities $\bar{v} \ll 1$, the cases of the Coulomb attraction and repulsion become qualitatively different. In the attraction case ($\delta_1 = -1$) the equilibrium point exists only for $\bar{r}_1 > \rho_* = 3 \times 2^{-2/3} \approx 1.890$ (see Appendix). One readily verifies that the radial eigenfrequency $\bar{\omega}_\parallel$ vanishes at $\bar{r}_1 = \rho_*$ in this case, and the condition (27) can never be fulfilled. The latter implies that $\bar{b}_{ad} \to \rho_*$ for $\delta_1 = -1$ and $\bar{v} \to 0$. In slow collisions with impact parameters $\bar{b} < \rho_*$ the electron is temporarily captured by the projectile and performs one or more revolutions around it before it is recaptured by the oscillator potential.

In the repulsive case ($\delta_1 = +1$) non-adiabatic collisions occur at $\bar{r}_1 = \bar{b}/\sin\theta \ll 1$. Expanding equations (25–28) with respect to this small parameter and retaining the first non-vanishing terms, we get

$$\bar{\omega}_\parallel^2 = 3, \qquad \bar{\omega}_\perp^2 = \bar{r}_1 = \frac{\bar{b}}{\sin\theta}, \tag{30}$$

$$\mu_\parallel = \frac{\bar{v}^2}{3\bar{b}^2}\,\sin^4\theta, \quad \mu_\perp = \frac{2\bar{v}^2}{\bar{b}^3}\,\sin^4\theta|\cos\theta|. \tag{31}$$

Equation (31) implies that the adiabaticity is first violated along the transverse normal coordinate, where the eigenfrequency $\bar{\omega}_\perp$ becomes small. More precisely, with the decreasing $\bar{b}$, parameter $\mu_\perp$ is the first to reach unity at $\sin^2\theta = 4/5$ and $\bar{b} = (4/5)^{5/6}\,\bar{v}^{2/3}$. From this we conclude that, for $\bar{v} \ll 1$, the adiabatic impact parameter $\bar{b}_{ad}$ is given by

$$\bar{b}_{ad} = \begin{cases} \bar{v}^{2/3}, & \delta_1 = +1, \\ 3 \times 2^{-2/3} = 1.890, & \delta_1 = -1. \end{cases} \tag{32}$$

6 Energy transfer $\mathsf{T}(\mathsf{v}, \mathsf{b})$ in a single collision

To calculate the stopping cross-section $\bar{S}_\pm(\bar{v})$ as a function of the projectile velocity $\bar{v}$, one needs to know the energy transfer $\bar{T}_\pm(\bar{v}, \bar{b})$ as a function of two variables $\bar{v}$ and $\bar{b}$. Below it is shown that a scaling law

$$\bar{T}_+(\bar{v}, \bar{b}) = \bar{v}^{1/3}\,\Phi_+(\bar{b}\bar{v}^{-2/3}) \tag{33}$$

can be established for $\bar{v} \ll 1$ in the case of the repulsive interaction; here $\Phi_+(\xi)$ is a function of a single variable ξ.

6.1 Scaling law for the repulsion case

By analogy with the case of $\bar{v} \gg 1$, one can assume that at low velocities the energy transfer in adiabatic collisions drops exponentially with $\bar{b}$, i.e. $\bar{T}_+ \propto \exp(-C\bar{b}/\bar{b}_{ad}) \propto \exp(-C\bar{b}\bar{v}^{-2/3})$, where C is a constant of order 1 [Fig. 2a and Eq. (35) below confirm that this is indeed the case]. Hence, the range of impact parameters relevant for calculating $\bar{S}_+$ should scale as $\Delta\bar{b} \propto \bar{v}^{2/3}$. Then, one can surmise that in the limit of $\bar{v} \to 0$ the transferred energy $\bar{T}_+(\bar{v}, \bar{b})$ should asymptotically obey a scaling law of the form $\bar{T}_+/\bar{v}^a \to \Phi_+(\bar{b}\bar{v}^{-2/3})$, where $\Phi_+(\xi)$ is a certain function of one variable. Here we demonstrate that the exponent $a = 1/3$.

Consider a collision with an impact parameter $\bar{b} < \bar{b}_{ad} = \bar{v}^{2/3}$. For times $\bar{t} \lesssim -\bar{b}_{ad}/\bar{v} = -\bar{v}^{-1/3}$, before the projectile enters the "non-adiabatic sphere" $\bar{r}_1 = \bar{b}_{ad}$, the motion of the electron is adiabatic and follows closely the trajectory (22) of the e.p. Then, as the projectile passes the oscillator center at $\bar{x} = \bar{y} = 0$, the e.p. flips over

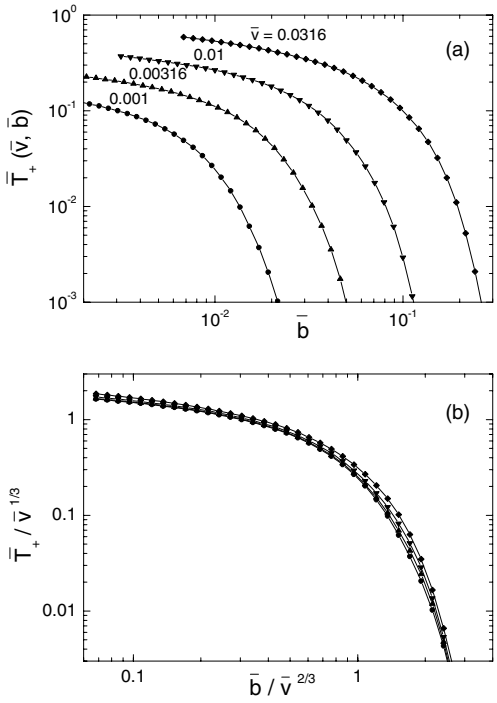

Fig. 2. (a) Energy transfer $\bar{T}_+$ in a single collision as a function of the impact parameter $\bar{b}$ calculated by integrating equations (16) for $\delta_1 = +1$ and four different values of the projectile velocity $\bar{v}$ [all quantities are in units (8)]. Each curve is marked by the corresponding value of the dimensionless velocity $\bar{v}$. (b) Same as (a) but in terms of the scaled quantity $\bar{T}_+/\bar{v}^{1/3}$ versus $\bar{b}/\bar{v}^{2/3}$.

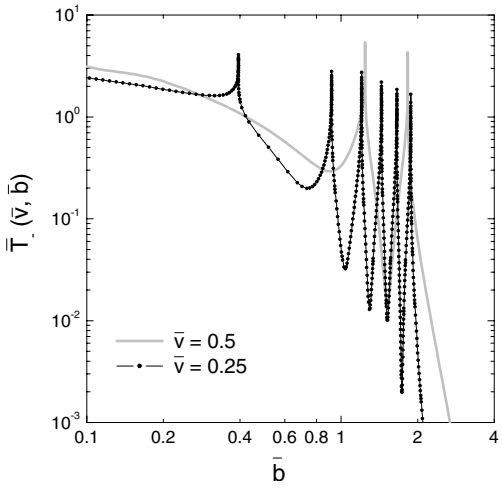

Fig. 3. Same as Figure 2a but for the case of the Coulomb attraction ($\delta_1 = -1$) for two values of the projectile velocity $\bar{v}$.

from $\bar{x}_{ep} \simeq +1$ to $\bar{x}_{ep} \simeq -1$ on a relatively short time scale $\Delta\bar{t} \simeq \bar{b}/\bar{v} < \bar{v}^{-1/3}$. In this phase the electron cannot adiabatically follow the e.p., and is left behind at $\bar{x} \simeq +1$: it moves over to a new position of the e.p. in a non-adiabatic manner on a longer time scale $\bar{t}_{na}$. One readily verifies that this time scale is $\bar{t}_{na} \simeq \bar{v}^{-1/3}$, and the non-adiabatic transition occurs along the transversal normal coordinate of local oscillations with the smaller eigenfrequency $\bar{\omega}_\perp \simeq \bar{b}_{ad}^{1/2} \simeq \bar{v}^{1/3}$. In the course of such a transition the electron acquires an oscillation velocity $\bar{v}_{e,na} \simeq 1/\bar{t}_{na} = \bar{v}^{1/3}$.

At the time $\bar{t} \gtrsim +\bar{b}_{ad}/\bar{v} = +\bar{v}^{-1/3}$ the collision enters the adiabatic phase again. By this time the electron is found in a time-dependent potential well, oscillating around the e.p. with a characteristic oscillation energy $\bar{E}_{e,na} \simeq \bar{v}_{e,na}^2 \simeq \bar{v}^{2/3}$. This oscillation energy is concentrated along the transversal normal coordinate with the eigenfrequency $\bar{\omega}_\perp \simeq \bar{b}_{ad}^{1/2} \simeq \bar{v}^{1/3}$. Note that the longitudinal eigenfrequency remains $\bar{\omega}_\parallel \simeq 1$ throughout all the collision phases. As the collision proceeds further, from $\bar{t} \simeq +\bar{v}^{-1/3}$ to $\bar{t} \simeq +\bar{v}^{-1}$, the eigenfrequency $\bar{\omega}_\perp$ is adiabatically restored from a small value $\bar{\omega}_\perp \simeq \bar{v}^{1/3}$ to $\bar{\omega}_\perp = 1$. During this second adiabatic phase, the ratio $\bar{E}_e/\bar{\omega}_\perp$ of the electron oscillation energy $\bar{E}_e$ to the corresponding eigenfrequency — being an adiabatic invariant of the one-dimensional oscillator ([7], § 49) — remains essentially constant. As a result, the energy transfer $\bar{T}_+$, equal to the final value of the electron oscillation energy $\bar{E}_{e,\infty}$, is given by

$$\bar{T}_+ = \bar{E}_{e,\infty} \simeq \bar{E}_{e,na}/\bar{v}^{1/3} \simeq \bar{v}^{1/3}, \tag{34}$$

which brings us to equation (33).

6.2 Numerical results for $\bar{\mathsf{T}}(\bar{\mathsf{v}}, \bar{\mathsf{b}})$

The scaling law (33) can be verified by direct numerical integration of equations (16). Figure 2 shows the results of such calculations for the repulsion case. One clearly sees how the widely separated curves for $\bar{T}_+(\bar{v}, \bar{b})$ from Figure 2a collapse upon a single limiting curve in Figure 2b when reduced to the scaled variables $\bar{T}_+/\bar{v}^{1/3}$ versus $\bar{b}/\bar{v}^{2/3}$. To an accuracy of 2–5% over the interval $0.1 < \bar{b}/\bar{v}^{2/3} < 2$, this limiting curve can be approximated as

$$\bar{T}_+(\bar{v}, \bar{b}) \approx 1.72\,\bar{v}^{1/3} \exp\left[-1.60\frac{\bar{b}}{\bar{v}^{2/3}} - 0.38\left(\frac{\bar{b}}{\bar{v}^{2/3}}\right)^2\right]. \tag{35}$$

A more detailed analysis reveals that, for a fixed velocity $\bar{v}$, the function $\bar{T}_+(\bar{v}, \bar{b})$ has a weak (logarithmic) singularity at $\bar{b} = 0$. This singularity is integrable and so weak that it is not visible in Figure 2; consequently, it has no practical effect on the value of the stopping cross-section $\bar{S}_+(\bar{v})$.

The case of the Coulomb attraction is qualitatively different from that of repulsion and more difficult to analyze. Figure 3 shows the plot of $\bar{T}_-(\bar{v}, \bar{b})$ calculated numerically for two values of $\bar{v} < 1$. One sees that the transferred energy exhibits characteristic resonances at certain values of the impact parameter $\bar{b}$. In the limit of $\bar{v} \to 0$, the first resonance occurs at $\bar{b} = \rho_* = 3 \times 2^{-2/3}$ (see Appendix). The resonances occur each time the number of revolutions of the electron around the projectile, when temporarily captured by its Coulomb field, increases by one. With the decreasing velocity $\bar{v}$, the number of resonances increases in

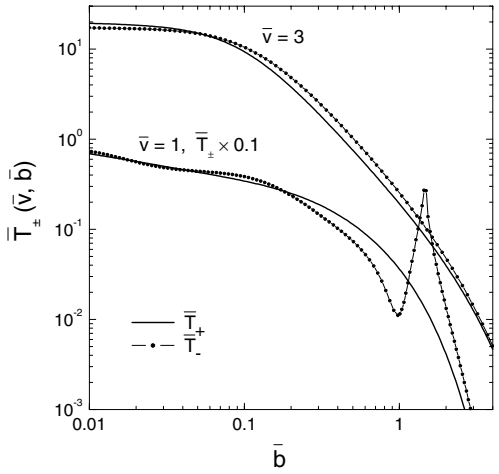

Fig. 4. Comparison of $\bar{T}_+(\bar{v},\bar{b})$ with $\bar{T}_-(\bar{v},\bar{b})$ for two values of $\bar{v} = 1$ and 3. For convenience of representation the values of $\bar{T}_\pm$ for $\bar{v} = 1$ are multiplied by a factor of 0.1.

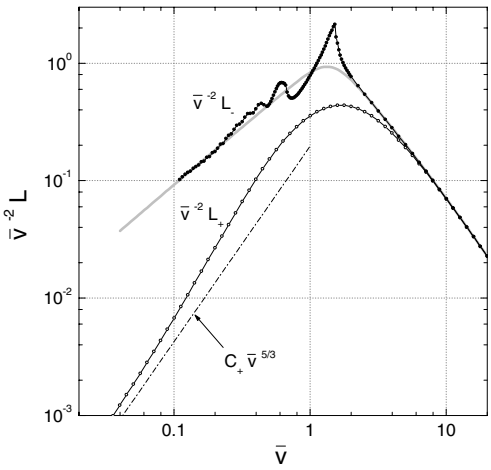

Fig. 5. Velocity dependence of the Bohr stopping cross-section. Plotted are the two dimensionless functions $(4\pi)^{-1}\bar{S}_\pm(\bar{v}) = \bar{v}^{-2}\,L_\pm(\bar{v})$. Dots on the curves correspond to actual values calculated by solving the equations of motion (16). Dash-dotted line is the asymptotic dependence (36). Thick grey curve is the fitting formula (40).

inverse proportion to $\bar{v}$, and each particular resonance becomes more narrow. As a consequence, direct calculation of the corresponding stopping cross-section S_- by numerically solving equations (16) becomes increasingly difficult for $\bar{v} \lesssim 0.1$.

Figure 4 shows a direct comparison of $\bar{T}_+(\bar{v},\bar{b})$ with $\bar{T}_-(\bar{v},\bar{b})$ for two values of the projectile velocity $\bar{v} = 1$ and 3. This plot gives an idea what range of the impact parameters gives the main contribution to the Barkas effect (see Sect. 8 below). At high velocities, $\bar{v} \gg 1$, the difference between $\bar{S}_+(\bar{v})$ and $\bar{S}_-(\bar{v})$ is practically uniformly accumulated over the entire interval $\bar{v}^{-2} \lesssim \bar{b} \lesssim \bar{v}$ contributing to the Bohr value (11) of the Coulomb logarithm, which is clearly manifested by the $\bar{T}_\pm(\bar{b})$ curves for $\bar{v} = 3$. At low velocities, $\bar{v} < 1.52$, the main contribution to the Barkas effect comes from the vicinity of resonances in the $\bar{T}_-(\bar{b})$ dependence, as demonstrated by the $\bar{v} = 1$ curves in Figure 4.

7 Stopping cross-section

7.1 The repulsion case

The scaling law (33) implies that the Bohr stopping cross-section S_+ for repulsively interacting projectile and bound electron becomes proportional to $v^{5/3}$ as $v \to 0$, namely

$$\bar{S}_+(\bar{v}) \to 4\pi\, C_+\, \bar{v}^{5/3}, L_+(\bar{v}) \to C_+\, \bar{v}^{11/3}, \qquad (36)$$

where C_+ is a constant. By integrating equation (35) we obtain a value of $C_+ \approx 0.1995$. Direct calculation of $\bar{S}_+(\bar{v})$ by numerically integrating equations (16) down to $\bar{v} = 10^{-3}$ yields

$$C_+ = 0.197 \pm 0.001. \qquad (37)$$

Figure 5 shows the function $\bar{v}^{-2}L_+(\bar{v}) = (4\pi)^{-1}\bar{S}_+(\bar{v})$ versus $\bar{v}$ as calculated by solving equations (16). It has a broad maximum around $\bar{v} = 1.7$ and falls off approximately as $\bar{v}^2$ towards smaller $\bar{v}$ over the range $0.04 \lesssim \bar{v} \lesssim 0.4$. The asymptotic law (36) is approached at significantly smaller velocity values $\bar{v} < 0.01$ (not shown in Fig. 5), which appear to be of little practical interest.

Since the Bohr stopping number L_+ is a universal function of $\bar{v}$ only, a simple fitting formula for it might be of practical interest. As such, the following formula is offered here

$$L_+(\bar{v}) \approx \frac{\ln(C_{+1} + C_B\bar{v}^3)}{1 + (3\pi/2)\,\bar{v}^{-3} + 2.36\,\bar{v}^{-4}\exp(-5\bar{v}^2)}. \qquad (38)$$

This expression is designed in such a way as (i) to reproduce accurately both the Bohr limit and the polarization correction (42) (see Sect. 8 below) with the value of constant

$$C_{+1} = \frac{3\pi}{2}\,C_B\,\ln\frac{C_B}{C_A} \approx 6.5528, \qquad (39)$$

and (ii) to yield $\bar{S}_+(\bar{v}) \propto \bar{v}^2$ at $\bar{v} \ll 1$; equation (38) deviates from the numerical results for $\bar{v} > 0.04$ by no more than 3%.

7.2 The attraction case

For the practically more important case of the attractive interaction ($\delta_1 = -1$), no asymptotic scaling law, similar to equation (33), has been found. The numerical results shown in Figure 5 indicate that the Bohr stopping cross-section $\bar{S}_-(\bar{v})$ appears to be not an analytic function of $\bar{v}$ at $\bar{v} < 2$: it exhibits a sharp maximum at $\bar{v} = 1.52$, followed by decaying oscillations towards smaller values of $\bar{v}$. The mountain-peak maximum occurs when the first sharp resonance appears on the curve $\bar{T}_-(\bar{b})$ (see Fig. 3). A similar local maximum — although not so sharp and at a smaller value of $\bar{v} \simeq 0.64$ — has also been observed by the authors of reference [8] within the binary theory

of electronic stopping. At $0.1 < \bar{v} < 1$, the Bohr stopping cross-section $\bar{S}_-(\bar{v})$ turns out to be very nearly proportional to the projectile velocity $\bar{v}$.

Similarly to the repulsion case, a fitting formula can be proposed for $L_-(\bar{v})$,

$$L_-(\bar{v}) \approx \left(1 + \frac{3\pi}{2}\,\bar{v}^{-3}\frac{1.2+\bar{v}}{1+\bar{v}}\right)\,\ln\left(1+\frac{C_B\bar{v}^6}{C_{-1}+\bar{v}^3}\right), \tag{40}$$

which for

$$C_{-1} = C_B^{-1} + \frac{3\pi}{2}\,\ln\frac{C_B}{C_A} = 6.7696 \tag{41}$$

reproduces exactly the first two terms of the asymptotic expansion (42) for $\bar{v} \gg 1$, and yields $\bar{S}_-(\bar{v}) \propto \bar{v}$ at $\bar{v} \ll 1$, as indicated by the numerical results. Interpolation (40) is, of course, smooth and deviates significantly from the "true" values of $L_-(\bar{v})$ near the sharp maximum of the latter (see Fig. 5).

8 Barkas effect

The difference between S_+ and S_- (or between L_+ and L_-) is usually called the Barkas effect [5,8]. Ashley et al. [9] calculated the functional form of the Barkas correction for the Bohr model in the limit of $\bar{v} \gg 1$, namely,

$$L_\pm(\bar{v}) = \ln\left(C_B\bar{v}^3\right) - \delta_1\frac{3\pi}{2}\bar{v}^{-3}\ln\left(C_A\,\bar{v}^3\right), \tag{42}$$

but the value of constant C_A was not determined. In reference [9] the perturbative method of Bohr was extended to the next order with respect to the displacement of the harmonically bound electron. Hence, the result of Ashley et al. yields the second (after the first one of Bohr) term in the asymptotic expansion of $L_\pm(\bar{v})$ for $\bar{v} \gg 1$, which may be called a polarization correction.

The present numerical results shown in Figure 5 agree perfectly with the polarization correction of Ashley et al., and are accurate enough to determine the value of C_A. Figure 6 shows the plot of the quantity

$$C_A(\bar{v}) = \bar{v}^{-3}\exp\left[\bar{v}^3\,(L_- - L_+)/3\pi\right], \tag{43}$$

which, according to equation (42), must approach a constant value at $\bar{v} \gg 1$. One sees that this is indeed the case, and that

$$C_A = 0.3255 \pm 0.001. \tag{44}$$

The error in equation (44) stems from computational errors of $\delta L/L \simeq 10^{-6}$ for the $L_\pm$ values.

From Figure 5 one can infer that, apart from strong fluctuations at $0.5 \lesssim \bar{v} \lesssim 2$, the ratio L_-/L_+ increases monotonically with the decreasing velocity $\bar{v}$. At $\bar{v} = 1.52$, where $\bar{S}_-$ is maximum, we have $L_-/L_+ = 4.9$.

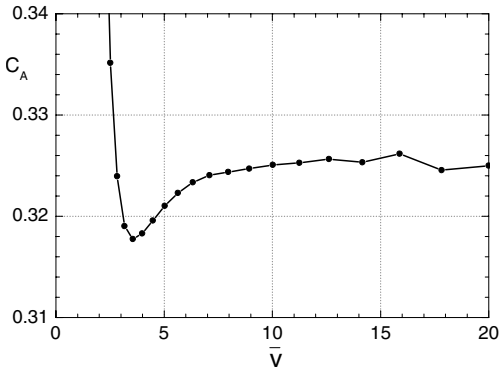

Fig. 6. Function $C_A(\bar{v})$, as defined by equation (43), is plotted by using numerical values of $L_\pm(\bar{v})$. As $\bar{v} \to \infty$, $C_A(\bar{v})$ should approach the value of constant C_A in the polarization correction (42) of Ashley et al. [9].

9 Discussion

There are two major restrictions for applicability of the Bohr model, namely (i) quantum effects, and (ii) finite ionization energies of atomic electrons. Constraints due to a finite ionization threshold I can be evaluated by assuming that the radius of action of the oscillator binding force is restricted by the value $r_a \simeq (I/m\omega^2)^{1/2}$. For the repulsive interaction, ionization at $\bar{v} \ll 1$ remains classically forbidden for all impact parameters under the condition that $Z_1e^2/r_a^2 < m\omega^2 r_a$. The latter means that the applicability of the Bohr model at low velocities is limited by the condition

$$I \gtrsim \left(Z_1^2e^4m\omega^2\right)^{1/3}. \tag{45}$$

Since typically $I \simeq \hbar\omega$, equation (45) is equivalent to a more transparent condition $I \gtrsim Z_1^2\mathrm{Ry}$. This condition applies to the attraction case as well. It is satisfied, for example, for the stopping of low-Z projectiles on K-shells of high-Z target elements.

The importance of the quantum effects at $v \lesssim v_s$ cannot be judged on the basis of condition (3), obtained for the Rutherford scattering of free charges. Instead, the condition

$$\bar{\hbar} \equiv \frac{\hbar\omega}{mv_s^2} = \frac{\hbar v_s}{|Z_1e^2|} = \frac{\hbar\omega}{\left(Z_1^2e^4m\omega^2\right)^{1/3}} \ll 1 \tag{46}$$

must be used. This condition ensures that the de Broglie wavelength $\lambda \simeq (\hbar/m\omega)^{1/2}$ of the electron in the ground state of an oscillator is small compared to its displacement ($\simeq b_s$) during a slow collision.

The only published results of non-perturbative quantum calculations [10] correspond to a fixed value of the parameter $2mv^2/\hbar\omega = 10$, and to an interval $0.1 < \alpha_v < 10$ of the values of $\alpha_v = |Z_1e^2|/\hbar v$. A limited comparison that can be made by using the plots in Figure 4 of reference [10] indicates that for $\bar{\hbar} \approx 1$ ($\bar{v} \approx 2$) the quantum values of $L_\pm$ are 30–40% below the corresponding classical ones. At the same time, the ratio L_-/L_+ appears to be rather insensitive to the quantum effects.

Once we notice that $\hbar\omega \simeq I$, we find that condition (46) is the opposite of inequality (45). This means

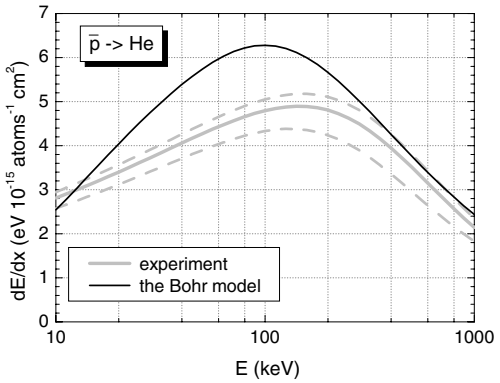

Fig. 7. Comparison with the experimental data from reference [11] for the Coulomb stopping of antiprotons in helium. Solid black curve: the Bohr model with $\hbar\omega = 42.3$ eV. Solid grey curve: the best fit to the experimental stopping power as given in reference [11]. Dashed grey curves indicate the error corridor for the experimental data.

that the low-velocity limit of the classical Bohr model is, strictly speaking, never applicable because of either target ionization or quantum effects.

The above conclusion does not mean, however, that the results of the Bohr model for $v < v_s$ are completely useless. First of all, in the absence of comprehensive quantum results, the Bohr stopping power may serve as a good starting (and/or a reference) point. Second, although the parameter $\bar{\hbar}$ is not small in practically interesting cases, neither is it always large. As a good characteristic example, the stopping of antiprotons in a helium gas may be considered. At low projectile velocities, antiprotons (and other antinuclei) are particularly interesting from the theoretical point of view because they do not participate in charge exchange events. Helium as a target material is also of special interest because (i) it has bound electrons in only a single atomic shell, and (ii) cannot be ionized by antiprotons in the limit of $v \to 0$ (at least from the classical point of view).

Figure 7 compares the Bohr stopping power, calculated by using equation (38) for L_+, with the experimental data for antiprotons in a helium target [11] at velocities corresponding to $E > 10$ keV/u, where the contribution of the nuclear stopping is still negligible. When applying the Bohr model, the same value of the oscillator frequency, $\hbar\omega = \hbar\langle\omega\rangle = 42.3$ eV, was used as in the limit of high projectile velocities [12]. This value corresponds to $\bar{\hbar} = 1.16$.

In Figure 7 it is seen that the prediction of the Bohr model is in a reasonable agreement with the experimental data: the difference between the two curves does not exceed 20–30%. Moreover, within the energy range 10 keV $< E <$ 60 keV, the dependence of the Bohr stopping power on the projectile velocity v is practically indistinguishable from the velocity-proportional law, $S \propto v$, whereas the experimental results of reference [11] deviate significantly from it. Since later experiments for antiproton stopping in other materials [13] have universally confirmed the velocity-proportional law, more accurate measurements of the antiproton stopping in helium may, in fact, show a better agreement with the Bohr model then the data in Figure 7.

The author is grateful to Prof. J. Meyer-ter-Vehn for many stimulating discussions, and for providing an opportunity to have a productive and pleasant visit to the Max-Planck-Institute for Quantum Optics (Garching, Germany). This work was supported by the Gesellschaft für Schwerionenforschung (Darmstadt) under the project MM-MTV, and by the INTAS grant 01-0233.

Appendix

Equation (24), when rewritten as

$$\varphi(\rho + \varphi)^2 = \delta_1, \tag{A.1}$$

defines two functions $\varphi(\rho)$, namely $\varphi_+(\rho) > 0$ and $\varphi_-(\rho) < 0$, depending on whether $\delta_1 = +1$ or -1. From physical considerations, we are interested in the solution of equation (A.1) which has the limiting behaviour

$$\varphi(\rho, \delta_1) = \frac{\delta_1}{\rho^2} - \frac{2}{\rho^5} + \ldots, \quad \rho \gg 1. \tag{A.2}$$

The function $\varphi_+(\rho)$ is defined for all $0 \le \rho < \infty$, and is given by the corresponding root of the cubic equation (A.1), namely

$$\varphi_+(\rho) = (P+Q)^{1/3} + (P-Q)^{1/3} - \frac{2}{3}\rho, \tag{A.3}$$

where

$$P = \frac{1}{2} + \left(\frac{\rho}{3}\right)^3, \quad Q = \left[\frac{1}{4} + \left(\frac{\rho}{3}\right)^3\right]^{1/2}. \tag{A.4}$$

For small ρ one has

$$\varphi_+(\rho) = 1 - \frac{2}{3}\rho + \frac{\rho^2}{9} + \ldots, \quad \rho \ll 1. \tag{A.5}$$

For $\delta_1 = -1$ the required solution of equation (A.1) is given by

$$\varphi_-(\rho) = -\frac{2}{3}\rho\left(1 - \cos\frac{\Theta}{3}\right), \tag{A.6}$$

where

$$\cos\Theta = 1 - \frac{1}{2}\left(\frac{3}{\rho}\right)^3. \tag{A.7}$$

This solution exists only for

$$1.890 \approx 3 \times 2^{-2/3} = \rho_* \le \rho < \infty. \tag{A.8}$$

Near $\rho = \rho_*$ the expansion of $\varphi_-(\rho)$ has the form

$$\varphi_-(\rho) = \varphi_* + \frac{2^{2/3}}{\sqrt{3}}(\rho - \rho_*)^{1/2} + \ldots, \quad 0 \le \rho - \rho_* \ll 1, \tag{A.9}$$

where $\varphi_* = -2^{-2/3} \approx -0.630$.

References

1. N. Bohr, Philos. Mag. **25**, 10 (1913)
2. H. Bethe, Ann. Physik **5**, 325 (1930)
3. F. Bloch, Ann. Physik **16**, 285 (1933)
4. P. Sigmund, Phys. Rev. A **54**, 3113 (1996)
5. J. Lindhard, Nucl. Instrum. Meth. **132**, 1 (1976)
6. *Handbook of Mathematical Functions*, edited by M. Abramowitz, I.A. Stegun (National Bureau of Standards, Washington D.C., 1972)
7. L.D. Landau, E.M. Lifshitz, *Mechanics* (Pergamon Press, Oxford, 1976)
8. P. Sigmund, A. Schinner, Nucl. Instrum. Meth. B **212**, 110 (2003)
9. J.C. Ashley, R.H. Ritchie, W. Brandt, Phys. Rev. B **5**, 2393 (1972)
10. H.H. Mikkelsen, H. Flyvbjerg, Phys. Rev. A **45**, 3025 (1992)
11. M. Agnello et al., Phys. Rev. Lett. **74**, 371 (1995)
12. S.P. Ahlen, Rev. Mod. Phys. **52**, 121 (1980)
13. S.P. Møller, A. Csete, T. Ichioka, H. Knudsen, U.I. Uggerhøj, H.H. Andersen, Phys. Rev. Lett. **88**, 193201 (2002)